VIII-Ⅱ-1. Project Research

Project 3

PR3 Project Research on Science and Engineering of Unstable Nuclei and Their Uses on Condensed Matter Physics

Y. Ohkubo

Research Reactor Institute, Kyoto University

Objective and Participating Research Subjects

The main objectives of this project research are the investigation of the nuclear structure of unstable neutron-rich nuclei and also the local properties of materials using short-lived nuclei.

This period is the second year of the project.

The research subjects (PRS) executed in this period are as follows:

PRS-1 Extension of usable fission products at KUR-ISOL
PRS-2 Determination of γ-ray intensities and evaluation of β-branching ratios for the decay of ^{147}La to ^{147}Ce.
PRS-3 Half-life measurements of excited levels in ^{149}Pr.
PRS-4 (a) Dynamic perturbation to ^{111}Cd(←^{111}Ag) doped in AgI nanoparticles; (b) Sites of impurities (^{140}Ce) implanted in Fe.
PRS-5 (a) Dispersion state of Al and Cd impurities in ZnO; (b) Irradiation effect on the formation of defects in ^{57}Co-doped ZnO observed by the Mössbauer spectroscopy.
PRS-6 Mössbauer study of a parent material of Fe-based superconductors, FeTe.
PRS-7 Study on rapid spin equilibrium and magnetic phase transition for $(C_6H_5)_4P[Mn^{II}Fe^{III}(C_2O_3S)_3]$ by means of high field ^{57}Fe Mössbauer spectroscopy.
PRS-8 Elucidation of a correlation between magnetic properties and host-guest interactions in porous coordination polymers.
PRS-9 Characterization of gold clusters supported on zinc oxide by ^{197}Au Mössbauer spectroscopy.
PRS-10 ^{129}I Mössbauer spectroscopy of AgI nanoparticles.

Main Results and Contents of This Report

In order to extend usable radioactive ion beams at KUR-ISOL, A. Taniguchi *et al*. (PRS-1) searched for neutron-rich Sr and Y isotopes and have observed ^{99}Sr with a half-life $t_{1/2}$ of 269 ms (the shortest among the nuclides extracted at KUR-ISOL) and ^{101}Y.

For ^{147}La(→^{147}Ce) obtained at KUR-ISOL, Y. Shima *et al*. (PRS-2) determined the values of 244 relative I_γs and 82 I_βs, using a coaxial 60% HPGe detector. They reevaluated the value of I_β for ^{147}La→^{147g}Ce to be 18%.

For ^{149}Ce(→^{149}Pr) obtained at KUR-ISOL, Y. Kojima *et al*. (PRS-3) measured the $t_{1/2}$s of the 58.2-keV and 125.6 keV levels in ^{149}Pr, using a radiation detection system consisting of a high-purity Ge detector, a thin plastic scintillator and a $LaBr_3$ one.

Using the excited level with a nuclear spin I = 5/2 and $t_{1/2}$ = 85 ns of ^{111}Cd(←^{111}Ag), W. Sato *et al*. (PRS-4a) observed a dynamic perturbation pattern in the TDPAC spectrum for AgI nanoparticles coated with a polymer (PVP) at room temperature, implying a hopping motion of Ag in AgI, while no perturbation was observed at room temperature for AgI with no polymer. Using the excited level with I = 4 and $t_{1/2}$ = 3.5 ns of ^{140}Ce(←^{140}La ←^{140}Ba←^{140}Cs), Y. Ohkubo *et al*. (PRS-4b) obtained the TDPAC result that about 30% of ^{140}Ce implanted in Fe occupy the substitutional Fe sites with no lattice defects nearby and feel the unique static magnetic hyperfine field.

Using the excited level of ^{111}Cd(←^{111m}Cd), S. Komatsuda *et al*. (PRS-5a) obtained the TDPAC result that Cd ions doped in ZnO disperse and reside solely at the substitutional Zn sites, while Al ions disperse in ZnO in the form of considerably large aggregates of their own. W. Sato *et al*. (PRS-5b) incorporated defects in ^{57}Co-doped ZnO by electron beam irradiation at KURRI-LINAC and found no indication of magnetism which might be induced in ZnO in the ^{57}Fe Mössbauer spectrum for the irradiated ZnO.

S. Kitao *et al*. (PRS-6) took ^{57}Fe Mössbauer spectra for $FeTe_{0.9}$ in a temperature range between 5 K and 290 K and obtained the result indicating the existence of a structural phase transition accompanied by a magnetic transition.

N. Kojima *et al*. (PRS-7) obtained the temperature and magnetic field dependences of ^{57}Fe Mössbauer spectra for $(C_6H_5)_4P[Mn^{II}Fe^{III}(C_2O_3S)_3]$ (**1-mto**). They obtained the following results: Although **1-mto** undergoes magnetic phase transitions at 30 K and 23 K, the spin state of Fe(III) is paramagnetic above 23K, there being rapid equilibrium between the high and low spin states. Below 23 K, the spins of Fe(III) are ordered. The critical external magnetic field for the Fe(III) spin-flop transition is higher than 8 T.

M. Ohba *et al*. (PRS-6) synthesized Fe(II) porous coordination polymers (PCPs). Employing ^{57}Fe Mössbauer spectroscopy on the PCPs, they obtained the result among others that depending on the guest molecule, PCPs exhibit different magnetic behavior.

Applying XAS and ^{197}Au-Mössbauer spectroscopy to a study on gold nanoparticles supported on ZnO (H_2), H. Ohashi *et al*. (PRS-9) obtained the results that Zn is not reduced and that some Au exist as Au(0), forming relatively uniform clusters.

Yamamoto *et al*. (PRS-10) applied ^{129}I-Mössbauer spectroscopy at 13 K to obtain information of the chemical state of Ag in AgI nanoparticles coated with PVP. From the observation of the valence of iodine being different from -1, they considered that this valence change is due to an interaction between the surface of the nanoparticles and PVP, which may stabilize the high temperature phase involving in superionic conductivity.

PR3-1

Extension of Usable Fission Products at KUR-ISOL

A. Taniguchi, Y. Ohkubo, M. Tanigaki, M. Shibata[1] and Y. Kojima[1]

Research Reactor Institute, Kyoto University
[1]*Radioisotope Research Center, Nagoya University*

INTRODUCTION: At ISOL facilities in the world, a variety of radioisotope ion beams are produced using various nuclear reactions. The variety of usable RI beams is one of important characteristics of RI beam facilities. Here at KUR-ISOL (Kyoto University Reactor-Isotope Separator On-Line), we have been trying to extend usable RI beams. In a previous period, we successfully obtained beams of ^{97}Sr and ^{98}Sr, which have rather short life for ISOL coupled to a gas-jet system like ours [1]. Moreover, although indium isotopes had never been attempted to extract at KUR-ISOL and therefore their availability had not been known, extraction of $^{126\text{-}128}$In beams were also performed by careful tuning of an ion source and a mass-analyzing electromagnet [2]. In Fig.1 are plotted values of yield vs. half-life for thermal fission products of ^{235}U including a part of usable nuclei at KUR-ISOL. In this period, ^{99}Sr ($T_{1/2}$=269 ms) and ^{101,102}Y ($T_{1/2}$=448 ms and $T_{1/2}$=300 ms) were chosen as next candidates, and extraction of ^{99}Sr and $^{101,\,102}$Y was attempted.

EXPERIMENTS: The $^{235}UF_4$ target of 50 mg was irradiated at KUR-ISOL under 1 or 5 MW reactor operation. The fission products were transported using the He/N_2 gas-jet system to a surface-ionization type ion-source. Sr and Y were ionized and extracted in the form of Sr^+ and YO^+, and then mass-separated using an electromagnet and collected on an aluminized Mylar tape. The yields were measured by detecting representative γ-rays with a 30% Ge detector placed at an in-beam position. The optimal values of the magnetic field and the input power of the ion source were determined on the basis of the previous KUR-ISOL operation.

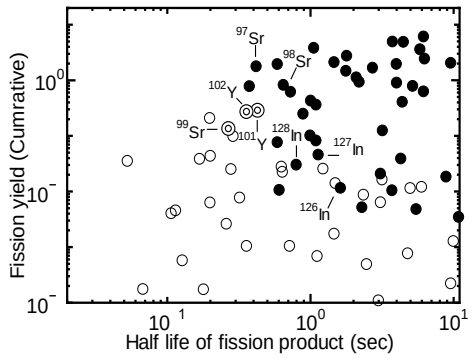

Fig.1 Yield vs. half-life for a part of the ^{235}U thermal fission products [3]. The filled circles represent the usable nuclei at KUR-ISOL and the open circles are for nuclei which have not yet extracted.

RESULTS and CONCLUSION: Fig. 2 shows the γ-ray energy spectra for the mass number A = 99 and for the background during the experiment. Representative γ-rays from ^{99}Sr and its descendant nuclides were observed. ^{99}Sr has become a nuclide having the shortest half-life among those observed at KUR-ISOL. Moreover, although a more detail analysis is required, γ-rays from ^{101}Y and its descent nuclides seem to have been observed in the A=101 energy spectrum. But, as for the A=102 spectrum, γ-rays from ^{102}Y were not clearly seen while γ-rays from ^{102}Nb were easily identified. This observation might be understood by invoking the facts that both the fission yield and the hale-life of ^{102}Nb are much larger than those of ^{102}Y. However, it is known that ionization of NbO is difficult in the case of using a surface ionization ion source. We therefore need to examine the observation carefully.

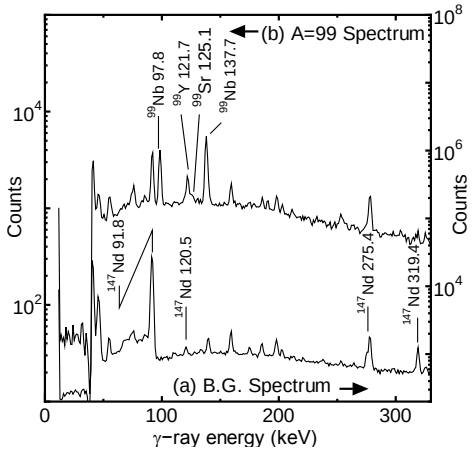

Fig.2 (a) Background γ-ray spectrum before the ion-beam is on. Mainly observed γ-rays are from ^{147}Nd ($T_{1/2}$=10.98 d) because an A=147 beam was used in other experiment before this experiment and the inside of the collection chamber was contaminated. (b) The γ-ray spectrum for A = 99. Representative γ-rays emitted in the decay of ^{99}Sr were observed. (The accumulation time of this spectrum was 1000 s.)

REFERENCES:

[1] A. Taniguchi *et al.*, KURRI Prog. Rep. **2010** (2011) 90.
[2] A. Taniguchi *et al.*, KURRI Prog. Rep. **2011** (2012) 172.
[3] T. R. England and B. F. Rider, LA-UR-94-3106, ENDF-349.

採択課題番号 24P3-1　オンライン同位体分離装置における生成核種の拡張と精密制御に関する研究　　プロジェクト

（京大・原子炉）谷口秋洋、大久保嘉高、谷垣　実（名大・RI センター）柴田理尋、小島康明

PR3-2 Determination of γ-Ray Intensities and Evaluation of β-Branching Ratios for the Decay of ^{147}La to ^{147}Ce

Y. Shima, H. Hayashi[1], Y. Kojima[2], A. Taniguchi[3] and M. Shibata[2]

Graduate School of Engineering, Nagoya University
[1]Institute of Health Biosciences, The University of Tokushima Graduate School
[2]Radioisotope Research Center, Nagoya University
[3]Research Reactor Institute, Kyoto University

INTRODUCTION: Decay schemes are essential information as nuclear data. In particular, those of fission products are important for studies of nuclear physics and engineering. For example, β- and γ-ray energies, γ-ray intensities I_γ and β-branching ratios I_β are necessary for decay heat calculations.

Until now, high energy excited levels and γ-ray transitions in ^{147}Ce and ^{145}La have been identified through the decay spectroscopy on ^{147}La and ^{145}Ba with a 4π clover detector [1]. In order to deduce these I_γ values, coincidence summing corrections based on the proposed decay schemes are necessary because of the large solid angle of the clover detector. In this study, to verify the correction, we measured γ-rays from the decay of ^{147}La in a far geometry and deduced the reliable I_γ as a reference. In addition, the I_β values for ^{147}La→^{147}Ce were also evaluated.

EXPERIMENTS: The intensities of γ-rays from ^{147}La were measured with a coaxial 60% HPGe detector. The detector was placed at 20 cm from a ^{147}La source. A 10-mm-thick plastic β-absorber was installed in front of the detector end cap. The detector was shielded with 5-mm-thick copper plates, 10-cm-thick lead blocks and boron-doped 5-cm-thick polyethylene blocks.

^{147}La isotopes were produced with neutron-induced fission of ^{235}U and mass-separated with KUR-ISOL. The mass-separated isotopes were collected on an aluminized Mylar tape and periodically transported to a measurement position. The tape cycle was set to be 8.0 s. Gamma-rays from ^{147}La were measured for 46 h.

The efficiency curve for the HPGe detector was determined using ^{152}Eu and ^{133}Ba. The efficiencies were also calculated with the Monte-Carlo simulation code GEANT4. The accuracy of the peak efficiencies was evaluated to be 1% from the difference between the experimental values and the calculated ones.

Using peak counts obtained from the singles spectrum and the peak efficiencies, I_γs for ^{147}La→^{147}Ce were deduced. The I_βs were calculated from the γ-ray intensity imbalance taking account of previously reported internal conversion coefficients.

RESULTS: In this experiment, 244 relative I_γs were determined for the decay of ^{147}La; 59 intensities were revised and 185 intensities were deduced for the first time. Fig. 1 shows the I_βs for ^{147}La→^{147}Ce. The open and closed bars represent previously reported values [2] and our present results, respectively. In this analysis, I_βs for 82 energy levels from 0 to 3045 keV were obtained. As shown in Table 1, the I_β for the decay to ^{147g}Ce decreases from 29% to 18% because I_βs for high energy levels were newly identified. Consequently, the log-*ft* value was evaluated to be 5.9.

CONCLUSIONS: We determined 244 relative I_γs for the decay of ^{147}La and I_βs for 82 levels in ^{147}Ce. The I_β for the ground state was reevaluated to be 18%. Measurements of high energy levels are necessary to determine accurately the I_β value for ^{147}La→^{147g}Ce. Compared to the present data, the data obtained with the clover detector have one order of magnitude better statistics. Demonstration of validity of the coincidence summing correction is now in progress.

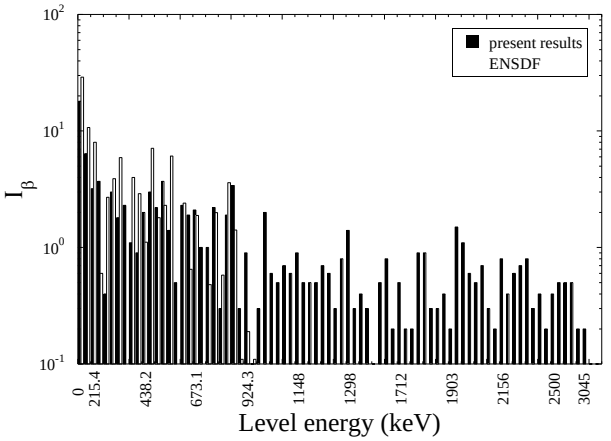

Fig.1. β-branching ratio I_β for ^{147}La→^{147}Ce. The values for the levels higher than 924.3 keV have been obtained for the first time.

Table 1. β-branching ratio I_β and log-*ft* value for ^{147}La→^{147g}Ce.

	present results	ENSDF
I_β (%)	18	29
log-*ft*	5.9	5.63

REFERENCES:

[1] Y. Shima *et al.*, Proc. Int. Conf. on Nuclear Data for Science and Technology 2013 (submitted).
[2] Evaluated Nuclear Structure Data File (ENSDF), http://nndc.bnl.gov/ensdf.

採択課題番号 24P3-2　全吸収検出器を用いた核分裂生成物の高励起準位の解明に向けた崩壊核分光研究　　プロジェクト

（名大・RIC）柴田理尋、小島康明（名大院・工）嶋　洋佑（徳島大・医）林　裕晃
（京大・原子炉）谷口秋洋

PR3-3

Half-Life Measurements of Excited Levels in ^{149}Pr

Y. Kojima, Y. Shima[1], H. Hayashi[2], A. Taniguchi[3] and M. Shibata

Radioisotope Research Center, Nagoya University
[1]Graduate School of Engineering, Nagoya University
[2]Institute of Health Biosciences, The University of Tokushima Graduate School
[3]Research Reactor Institute, Kyoto University

INTRODUCTION: Half-lives of nuclear excited levels are one of the most important nuclear data. For example, precise determination of the half-life is necessary for nuclear applications such as material science because it relates to the natural width of the level. Knowledge of the half-lives also makes it possible to determine the γ-ray reduced transition probabilities or nuclear matrix elements, which are useful for studying nuclear structure. Although half-life data provide valuable information to nuclear science, half-lives of only a limited number of levels in fission products have been measured because these nuclides are difficult to produce and most of the levels are short-lived.

To measure nuclear level half-lives down to sub-nanosecond, we have installed a spectrometer at the on-line isotope separator KUR-ISOL. To date, the half-lives of ^{148}Ce, ^{148}Pr and ^{149}Nd have been successfully measured using this apparatus [1,2]. In this report, we present our recent experimental results on ^{149}Pr.

EXPERIMENTS: The parent nuclide of ^{149}Pr, i.e. ^{149}Ce was prepared at KUR-ISOL, following the thermal neutron-induced fission of ^{235}U. The fission products were thermalized in the target chamber, and transported to a thermal ion source by gas jet stream. After ionization, the nuclides were extracted, accelerated to 30 keV, and mass-separated with a resolution of $M/\Delta M$~600. The mass-separated beams were implanted into an aluminum-coated Mylar tape, and periodically moved to the lead-shielded detector station.

At the detection port, we placed a $LaBr_3$ scintillator (1.5 × 1.5 inch), a 1-mm-thick plastic scintillator and a short-coaxial Ge detector. The level half-lives were measured by means of the β–γ–γ delayed coincidence technique. In this method, the time difference between β and γ detection was measured using a time-to-amplitude converter (TAC); The β signal from the plastic scintillator started the TAC unit, and the γ signal from the $LaBr_3$ stopped it. The Ge detector was used for selecting a desired γ transition branch through off-line sorting. The β–γ–γ coincidence data were recorded in list mode.

RESULTS: Fig. 1 shows two notable decay curves obtained for ^{149}Pr. Note that we analyzed the data based on the decay scheme reported in Refs. [3,4]. A slope is clearly observed in each figure. The half-life was deduced through the least-squares fitting method using a exponential function. The results are summarized in Table 1.

The half-life of 7.2(6) ns which we obtained for the 58.2-keV level is approximately consistent with the half-life of 10(2) ns reported in Ref. [4]. Our data has much improved the precision and reliability. This is because the time resolution of our spectrometer is superior to that in the previous work, in which a planar Ge detector was used as a timing γ detector. We also report the first measurements of the half-lives for the 86.5- and 125.6-keV levels, although the relative uncertainties are large due to low statistics.

SUMMARY: We measured level half-lives for ^{149}Pr including two first experimental results. These data should be indispensable in discussing the nuclear structure.

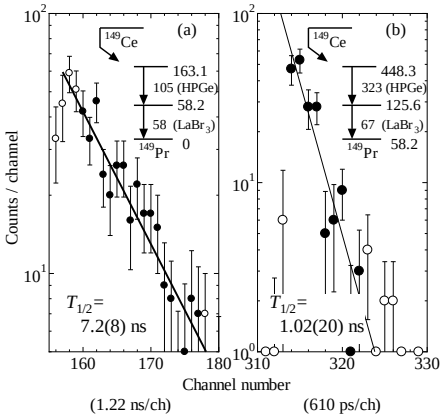

Fig. 1. Decay curves observed for (a) the 58.2-keV and (b) the 125.6-keV levels in ^{149}Pr. The energy gates used to obtain these decay curves are shown in the insets. The closed circles represent the fitting region.

Table 1. Half-lives obtained for the excited levels in ^{149}Pr .

Level	Gate (keV)		Half-life (ns)		
(keV)	$LaBr_3$	HPGe	Slope	Ave.	Ref.[4]
58.2	58.2	104.9	7.2(8)	7.2(6)	10(2)
58.2	58.2	172.6	7.1(10)		
86.5	86.5	76.5	4.0(8)	4.2(5)	—
86.5	86.5	129.1	4.3(7)		
125.6	67.4	322.5	1.0(2)	1.0(2)	—

REFERENCES:

[1] Y. Kojima *et al.*, Nucl. Instr. Meth., **A 659** (2011) 193-197.
[2] Y. Kojima *et al.*, Proc. Int. Conf. on Nuclear Data for Science and Technology 2013 (submitted).
[3] B. Singh, Nucl. Data Sheets 102 (2004)1-292.
[4] K. Yamauchi *et al.*, KURRI-KR-3, pp.51-53, (in Japanese).

採択課題番号 24P3-3　核分裂生成物に対する励起準位寿命測定を中心とした崩壊核分光　プロジェクト
（名大・RIC）小島康明、柴田理尋　（名大院・工）嶋　洋佑　（徳島大・医）林　裕晃
（京大・原子炉）谷口秋洋

PR3-4 Dynamic Perturbation to ^{111}Cd(←^{111}Ag) Doped in AgI Nanoparticles

W. Sato, R. Mizuuchi[1], S. Komatsuda[1], S. Kawata[2], A. Taoka and Y. Ohkubo[3]

Institute of Science and Engineering, Kanazawa University
[1]*Graduate School of Natural Science and Technology, Kanazawa University*
[2]*Department of Chemistry, Faculty of Science, Fukuoka University*
[3]*Research Reactor Institute, Kyoto University*

INTRODUCTION: It is well known that silver iodide (AgI) offers superionic conductivity as in its high-temperature α phase, and applications of this solid-state conductivity are desired in a wide field of industry. This conducting phenomenon, however, emerges at high temperature because of temperature-dependent crystal structures, which is indeed a barrier to practical applications of this compound.

Recently, an epoch-making technique was reported to break through this situation: AgI powder coated with poly-N-vinyl-2-pyrrolidone (PVP) can drastically enhance the ionic transport property at room temperature, recording the conductivity of 1.5×10^{-2} Ω^{-1} cm^{-1} [1]. The authors of Ref. [1] report that this achievement is due to successful control of the particle size as small as nanoscale. For a detailed understanding of ionic conductivity of this binary solid, it is of great importance to examine lattice-to-lattice hopping motion of Ag^+ ions on an atomic scale. For that purpose, in the present work, dynamic behavior of Ag^+ ions has been observed by means of the time-differential perturbed angular correlation (TDPAC) technique using the probe of ^{111}Cd(←^{111}Ag) nuclei. Here, preliminary results of successful observation of room-temperature dynamic motion of Ag^+ ions are reported.

EXPERIMENTS: For the production of the TDPAC probe, Pd foil was irradiated with thermal neutrons in Kyoto University Reactor. After radioequilibrium was achieved between ^{111}Pd and ^{111}Ag, the Pd foil was dissolved in HNO_3 aq. solution, and carrier-free ^{111}Ag was isolated by an anion exchange chromatography. The separated ^{111}Ag was incorporated in AgI samples when the powder sample was synthesized by precipitation. In the present work, two different AgI samples were prepared: PVP-free and PVP-coated. We confirmed by transmission electron microscopy that microscopic particles with sizes of 10-100 nm were synthesized for ^{111}Ag-free PVP-coated AgI.

TDPAC measurements of the ^{111}Cd(←^{111}Ag) probe were performed for both samples at various temperatures to observe temperature dependence of the spectra. The directional anisotropy, $A_{22}G_{22}(t)$, was deduced from the following relation:

$$A_{22}G_{22}(t) = \frac{2[N(\pi,t) - N(\pi/2,t)]}{N(\pi,t) + 2N(\pi/2,t)}. \qquad (1)$$

Here, A_{22} denotes the angular correlation coefficient, $G_{22}(t)$ the time-differential perturbation factor as a function of the time interval, t, between the relevant cascade γ-ray emissions, and $N(\theta, t)$ the number of the delayed coincidence events observed at an angle, θ.

RESULTS: For the PVP-free AgI polycrystals, no time variation is seen in the TDPAC spectrum at room temperature, which suggests that the ^{111}Cd(←^{111}Ag) probe duly occupies the tetrahedral lattice sites of Ag^+ in zinc blende crystal structure as in the γ phase. In the high-temperature (> 419 K) α phase, the TDPAC spectra show an exponential relaxation, signifying a dynamic perturbation on the probe nucleus.

As regards the PVP-coated AgI nanoparticles, on the other hand, typical dynamic perturbation was observed even at room temperature as shown in Fig. 1. The directional anisotropy of the spectrum shows a relaxation in the time scale of 10^{-7} s, which corresponds to nuclear relaxation time by the dynamic perturbation arising from fast fluctuation of the extranuclear charge distribution, namely, hopping motion of Ag^+ ions. It is considered that PVP-coating has made it possible for the α phase to survive at room temperature, realizing superionic conductivity.

For evaluating the hopping rate of Ag^+ ions, it is essential to obtain the value of nuclear quadrupole frequency as they are still at their lattice site. Experiments for the data acquisition are now in progress.

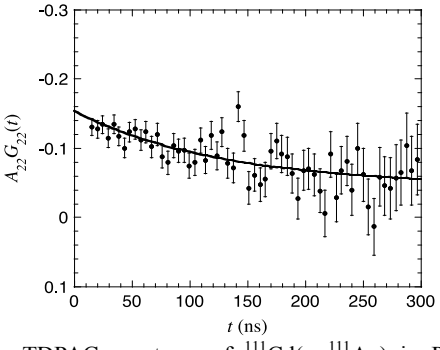

Fig. 1. TDPAC spectrum of ^{111}Cd(←^{111}Ag) in PVP-coated AgI at room temperature.

REFERENCE:

[1] R. Makiura *et al. Nature Mater.* **8**, (2009) 476 – 480.

採択課題番号 24P3-4a　超イオン伝導体 AgI 中の放射性核での電気四重極相互作用　プロジェクト（京大・原子炉）大久保嘉高、谷口秋洋、谷垣　実（金沢大・理工研究域）佐藤　渉（金沢大院・自然）水内理映子

PR3-5 Sites of Impurities (^{140}Ce) Implanted in Fe

Y. Ohkubo, A. Taniguchi, Q. Xu, and M. Tanigaki

Research Reactor Institute, Kyoto University

INTRODUCTION: Cerium does not form a solid solution with iron. It is interesting to examine where Ce ions occupy in Fe when they are implanted in it. If Ce ions reside in the substitutional sites, the nuclei of Ce should feel a large hyperfine magnetic field, B_{hf}. This time, we applied the time-differential perturbed angular correlation (TDPAC) technique to the 2083 keV state of ^{140}Ce implanted in Fe, and observed that about 35% of Ce felt a large hyperfine magnetic field, which in turn indicates that this amount of Ce ions are located at the substitutional sites. Incidentally, from the Larmor frequency, ω_L, measured with the TDPAC method and a reported value of the B_{hf} at ^{141}Ce in Fe, -41(2) T, we could derive the magnetic moment, μ, of the 2083 keV state of ^{140}Ce (see Ref. [1] about the obtained μ value and a comparison of it with two shell-model calculation results).

EXPERIMENTS: Room-temperature implantation of 100-keV ^{140}Cs ions was performed on an Fe foil at KUR-ISOL, and in a different run a similar implantation was done in order to check reproducibility. Each of the two Fe foils was 0.1-mm thick and of 99.995% purity, which had been annealed in H_2 atmosphere at 700°C for 2 h and polished. ^{140}Cs decays to ^{140}Ce through ^{140}Ba and then ^{140}La. We name these samples ^{140}Ce*Fe*.

The time dependences of the coincidence counts $N(\theta, t)$ of the 329-487 keV cascade γ rays accompanying the beta decay of ^{140}La in the two Fe samples were taken at room temperature with two measurement systems, each consisting of standard fast-slow electronic modules and four BaF_2 scintillation detectors. Here, θ and t denote the angle and the time interval, respectively, between the cascade γ rays. The directional anisotropy $A_{22}G_{22}(t)$ is obtained as follows:

$$A_{22}G_{22}(t) = 2\frac{N(180°,t) - N(90°,t)}{N(180°,t) + 2N(90°,t)}. \qquad (1)$$

RESULTS: In Fig. 1 are shown the two TDPAC spectra obtained for the two ^{140}Ce*Fe* samples. A clear oscillation pattern can be seen in both spectra, and the frequencies and amplitudes are identical with each other. As for the oscillation pattern, reproducibility has therefore been confirmed. From another TDPAC measurement on the 1st sample using three BaF_2 detectors (θ = ±135°) with an external magnetic field (B_{ext} = 0.3 T), we found that the oscillation pattern in Fig. 1 was due to the magnetic hyperfine interaction, since the oscillation pattern obtained with B_{ext} was reversed with the inversion of the external magnetic field. The amplitude of the oscillation, i.e., the effective A_{22} value (and the ω_L value) for the 1st sample are -0.042 (and +1927(7) Mrad/s) and those for the 2nd sample -0.051 (and +1930(8) Mrad/s). These amplitudes are much smaller than a reported A_{22} value of -0.13, indicating that only 30-40% of the ^{140}Ce implanted in Fe feel the unique static magnetic hyperfine interaction. This value is close to the fraction of Ce that was considered to occupy the substitutional Fe sites, 28.9(5)%, obtained in a nuclear orientation (NO) measurement on ^{141}Ce in Fe [2], although ^{141}Ce ions were directly implanted into an Fe foil, while in our case ^{140}Cs ions, ^{140}Ce's precursors, were implanted. In NO, the so-called two-site model is used, in which a fraction of impurity nuclei occupy "good sites", experiencing the full hyperfine interaction and the remainder zero interaction. Our A_{22} value may justify the use of the two-site model for ^{141}Ce*Fe* and implies that a same fraction of Cs, Ba and La also occupy "good sites" in Fe.

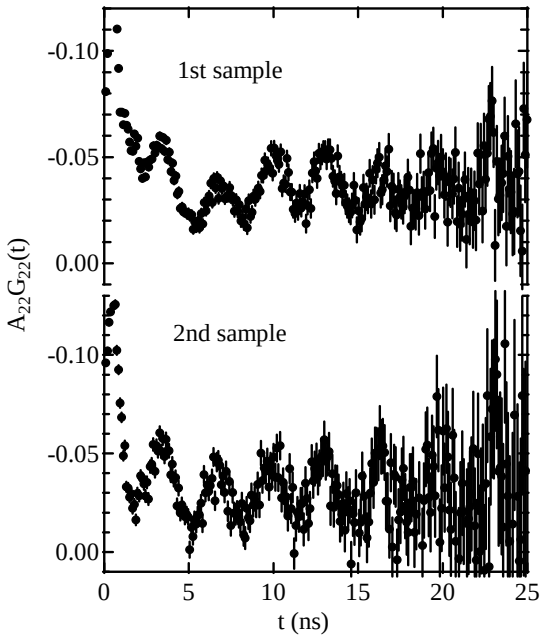

Fig. 1. Room-temperature TDPAC spectra for two samples of ^{140}Ce*Fe*.

REFERENCES:

[1] Y. Ohkubo, A. Taniguchi, Q. Xu, M. Tanigaki, N. Shimizu, and T. Otsuka, Phys. Rev. C **87**, 044324 (2013).

[2] W. van Rijswijk, F. G. van den Berg, H. E. Keus, and W. J. Huiskamp, Physica B+C **113**, 127 (1982).

採択課題番号 24P3-4b　超イオン伝導体 AgI 中の放射性核での電気四重極相互作用　プロジェクト（京大・原子炉）大久保嘉高、谷口秋洋、谷垣　実（金沢大・理工研究域）佐藤　渉（金沢大院・自然）水内理映子

PR3-6 **Dispersion State of Al and Cd Impurities in ZnO**

S. Komatsuda, W. Sato[1] and Y. Ohkubo[2]

Graduate School of Natural Science and Technology, Kanazawa University
[1]*Institute of Science and Engineering, Kanazawa University*
[2]*Research Reactor Institute, Kyoto University*

INTRODUCTION: Zinc Oxide (ZnO) doped with group 13 elements (Al, Ga, In) as impurity donors is expected to be applied to functional devices as n-type semiconductors. For a practical use of ZnO as a conduction-controlling device, it is of great importance to study the physical and chemical states of the dilute impurity ions in ZnO. The time-differential perturbed angular correlation method (TDPAC) is very suited for that purpose because it can directly provide atomic-level information of impurity atoms. In our previous TDPAC studies, the ^{111}Cd(←^{111m}Cd) probe has little interaction with Al atoms doped in ZnO even at a high concentration of 10 at.%, suggesting that Al impurities form some types of aggregate [1,2]. In order to confirm the above inference, a TDPAC study was performed for ZnO doped with Cd ions. Here, by a comparative study, more credible information on the Al state of being is presented.

EXPERIMENTS: For the synthesis of 2 at.% Cd-doped ZnO, stoichiometric amounts of cadmium oxide (CdO) and ZnO powder were mixed in a mortar for 2 h. The mixture was then pressed into a disk, and sintered in air at 1273 K for 3 h. About 3 mg of CdO enriched with ^{110}Cd was irradiated with thermal neutrons in a pneumatic tube at Kyoto University Reactor, and radioactive ^{111m}Cd was generated by ^{110}Cd(n, γ)^{111m}Cd reaction. The neutron-irradiated CdO powder was then added into the 2 at.% Cd-doped ZnO powder, and mixed again in a mortar for 20 min. The mixture was pressed into a disk, and sintered in air at 1373 K for 45 min. A TDPAC measurement was carried out for the ^{111}Cd(←^{111m}Cd) probe on the 151-245 keV cascade γ rays with the intermediate state of I = 5/2 having a half-life of 85.0 ns.

RESULTS: Fig. 1 shows the TDPAC spectra of ^{111}Cd(←^{111m}Cd) probe (a) in 2 at.% Cd-doped and (b) in 10 at.% Al-doped ZnO [2]. The directional anisotropy on the ordinate, $A_{22}G_{22}(t)$, was deduced from delayed coincidence events of the cascade:

$$A_{22}G_{22}(t) = \frac{2[N(\pi,t) - N(\pi/2,t)]}{N(\pi,t) + 2N(\pi/2,t)}.$$

Here, A_{22} denotes the angular correlation coefficient, t) the time-differential perturbation factor as a function of the time interval, t, between the relevant cascade γ-ray emissions, and $N(\theta,t)$ the number of the coincidence events observed at angle, θ. From our previous TDPAC measurement for undoped ZnO, it was found that the ^{111}Cd(←^{111m}Cd) probe uniformly disperses in ZnO and occupies the substitutional Zn site [3]. With respect to Fig. 1(a), the spectral damping appears as a result of distribution of the quadrupole frequency δ (= 12.2 (8)%). Because the distribution is an index of diversity of the vicinity surrounding the ^{111}Cd(←^{111m}Cd) probe, this experimental result shows that Cd ions are widely dispersed in ZnO. On the other hand, in Fig. 1(b), the spectral damping is less pronounced despite the presence of 10 at.% Al ions in the system (δ = 7.4 (7)%), suggesting that doped Al ions do not uniformly disperse in ZnO. We found from these observations that doped Cd ions diffuse into ZnO matrix and reside solely at the substitutional Zn site, while Al ions disperse in ZnO in the form of considerably large aggregates of their own.

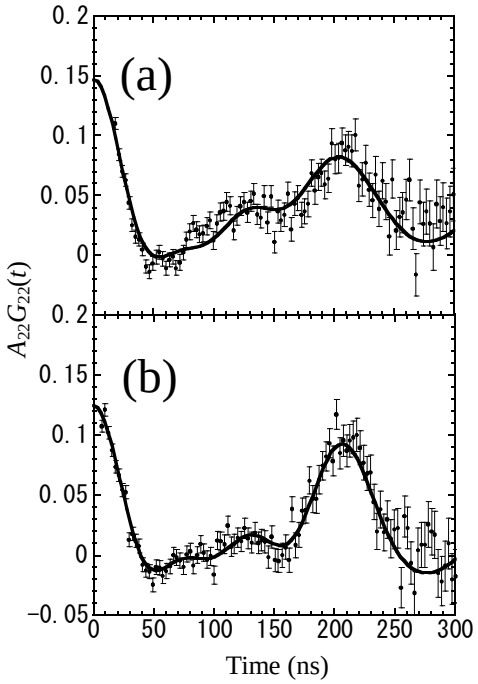

Fig. 1. TDPAC spectra of ^{111}Cd(←^{111m}Cd) (a) in 2 at.% Cd-doped and (b) in 10 at.% Al-doped ZnO.

REFERENCES:

[1] S. Komatsuda, W. Sato, S. Kawata, and Y. Ohkubo, J. Phys. Soc. Jpn. **80**, (2011) 095001.
[2] S. Komatsuda, W. Sato, and Y. Ohkubo, KURRI Progress Report **2010**, (2011) 94.
[3] W. Sato, S. Komatsuda, and Y. Ohkubo, Phys. Rev. B **86**, (2012) 235209.

採択課題番号 24P3-5a　　酸化亜鉛中の不純物が形成する局所構造観察　　プロジェクト
（金沢大・理工研究域）佐藤　渉（金沢大院・自然）小松田沙也加（京大・原子炉）大久保嘉高

PR3-7

Irradiation Effect on the Formation of Defects in ^{57}Co-Doped ZnO Observed by the Mössbauer Spectroscopy

W. Sato, T. Suzuki[1], Y. Kano[1], T. Takahashi[2], N. Abe[2] and Y. Ohkubo[2]

Institute of Science and Engineering, Kanazawa University
[1]*Graduate School of Natural Science and Technology, Kanazawa University*
[2]*Research Reactor Institute, Kyoto University*

INTRODUCTION: Zinc oxide (ZnO) is a promising *n*-type semiconductor having an optoelectronic property. It is also known that doping of a minute amount of magnetic element(s) such as Co, Fe, and Mn induces dilute magnetism in the semiconductor, leading to future spintronics devices. Apart from the impurity-induced magnetism, damages brought about by the kinetic implantation of impurity ions are also attracting attention as another cause of magnetism [1]. According to Ref. [1], the induced magnetism arises from lattice damages produced around the dopants substituting for Zn. However, there is another interpretation of the experimental result that the induced magnetism is ascribable to exchange interaction between impurity ions implanted at a high dose. Thus, the origin of the magnetism is not yet unequivocal. The purpose of the present work is to examine the irradiation effect on the hyperfine field produced by defects presumably formed around dilute magnetic ions doped in ZnO. In this work, we introduced in ZnO the ^{57}Co(→^{57}Fe) probe of the Mössbauer spectroscopy, and Mössbauer parameters obtained before and after electron beam irradiation are discussed.

EXPERIMENTS: Powder ZnO was pressed into a disc, and ^{57}Co HCl solution was then added in droplets onto the disc. For the diffusion of the radioactive ions, the sample was heated in air to perform a solid state reaction at 1273 K for 6 h. The prepared sample was ground into powder and measured by the emission Mössbauer spectroscopy with the ^{57}Co(→^{57}Fe) probe. After the spectrum was obtained, the sample was sealed in a quartz tube in vacuum, and irradiated for 30 m with electrons and bremsstrahlung of the maximum energy of 19 MeV. The average current of the pulsed electron beam at the sample was approximately 150 μA. After the irradiation, an emission Mössbauer measurement was again performed for the sample.

RESULTS: The Mössbauer spectra of ^{57}Co(→^{57}Fe) doped in ZnO measured at room temperature are shown in Fig. 1, and the Mössbauer parameters obtained by the fits are listed in Table 1. As shown in Fig. 1(a), the spectrum is made up of only one component exhibiting a quadrupole splitting. It was found from the Mössbauer parameters that ^{57}Co occupies the defect-free substitutional Zn site [1], where no internal magnetic field is present. For the Mössbauer measurement for the irradiated sample, as is obvious with Table 1, little change was observed in the hyperfine parameters. Besides, contrary to the inference from the reports [1,2], local magnetism was not induced by the present irradiation condition. This result implies the following two possibilities: 1) the local structure surrounding the probe is stable enough to preserve the chemical bonding from the present irradiation, or 2) although the local structure was indeed damaged once by the irradiation, annealing effect has worked to repair the damages because of the room temperature irradiation. For further information on the irradiation effect, low temperature irradiation and/or measurement should be carried out.

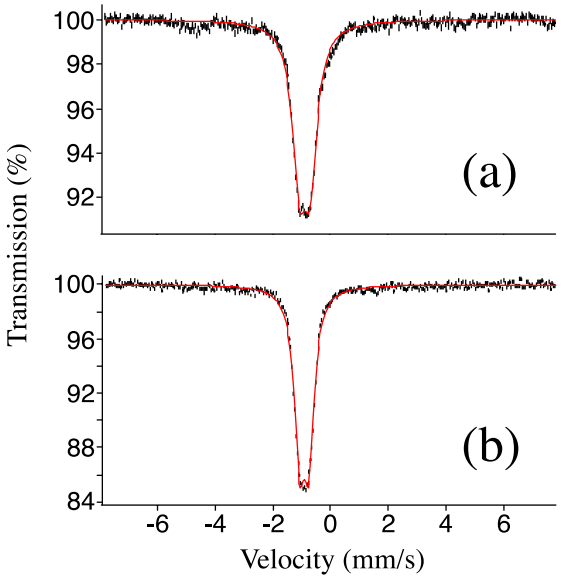

Fig. 1. Mössbauer spectra of ^{57}Co(→^{57}Fe) doped in ZnO measured at room temperature (a) before and (b) after irradiation with electrons and bremsstrahlung.

Table 1. Mössbauer parameters obtained for ^{57}Co-doped ZnO at room temperature. The alphabetical notation for the sample has the same meaning as that in Fig. 1.

Sample	I. S. (mm/s)	Q. S. (mm/s)	B_{hf} (T)
(a)	0.78 (1)	0.39 (1)	—
(b)	0.81 (1)	0.33 (1)	—

REFERENCES:

[1] G. Weyer *et al.*, *J. Appl. Phys.* **102** (2007) 113915 (1 – 7).
[2] R. Sielemann *et al.*, *Phys. Rev. Lett.* **101** (2008) 137206 (1 – 4).

採択課題番号 24P3-5b　　酸化亜鉛中の不純物が形成する局所構造観察　　プロジェクト
（金沢大・理工研究域）佐藤　渉（金沢大院・自然）小松田沙也加（京大・原子炉）大久保嘉高

PR3-8 Mössbauer Study of a Parent Material of Fe-Based Superconductors, FeTe

S. Kitao[1,2], M. Kurokuzu[1,2], Y. Kobayashi[1,2], R. Masuda[1], and M. Seto[1,2,3]

[1]*Research Reactor Institute, Kyoto University*
[2]*CREST, Japan Science and Technology Agency*
[3]*Japan Atomic Energy Agency*

INTRODUCTION: Since the discoveries of the Fe-oxipnictide superconductors, LaFePO [1] and $LaFeAsO_{1-x}F_x$ [2], extensive researches have been performed to elucidate the mechanism of their superconductivity. Among these and the successively discovered related Fe-based superconductors, the so-called "11" series, such as FeSe [3], has the simplest crystal structure. However, different from the firstly-found "1111" series, the magnetism of the parent compound of "11" series, FeTe, shows a complicated magnetic structure [4]. Since it is believed that the Fe acts as a key element and its magnetism must relate to the superconductivity, studies of their Fe magnetism is one of the main issues to reveal its superconducting mechanism. To investigate the nature of its magnetism, ^{57}Fe-Mössbauer spectroscopy is an essential method. Until today, a number of Mössbauer studies on these Fe-based superconductors have been carried out and revealed many important facts for $LaFeAsO_{1-x}F_x$ [5,6] and FeTe [7-9]. However, the complicated magnetism of FeTe has not thoroughly been understood yet. In this study, the magnetic structure of FeTe was investigated by obtaining detailed temperature dependence of the Mössbauer spectra.

EXPERIMENTS: A single crystal of $FeTe_{0.9}$ was synthesized from a stoichiometric mixture of reduced Fe and distilled Te in a crucible of aluminum oxide sealed in a quartz tube. The tube was heated up to 1070°C in 24 h and cooled down to 710°C at a rate of 3°C/h, and annealed at 400 °C for 10 days. The obtained single crystal was characterized by x-ray diffraction and magnetic susceptibility measurements. ^{57}Fe-Mössbauer spectra were measured using a pellet of powdered $FeTe_{0.9}$ using a ^{57}Co source in Rh matrix with a nominal activity of 1.85 GBq. The velocity scales are referenced to α-Fe.

RESULTS AND DISCUSSION: Typical Mössbauer spectra for $FeTe_{0.9}$ are shown in Fig. 1. The magnetic transition was clearly observed by the detailed temperature dependence of the Mössbauer spectra. The observed internal magnetic field reached around 10 T at 5K with a certain distribution, implying a complicated magnetic structure. The magnetic transition temperature was determined to be around 70 K by the temperature dependence of the internal magnetic fields. The observed anisotropy of the magnetic spectrum clearly indicates the existence of a quadrupole splitting in the magnetic ordered phase. Since the value of the quadrupole splitting abruptly changes from that for the high temperature phase, this change is considered to be due to a structural phase transition accompanied by the magnetic transition.

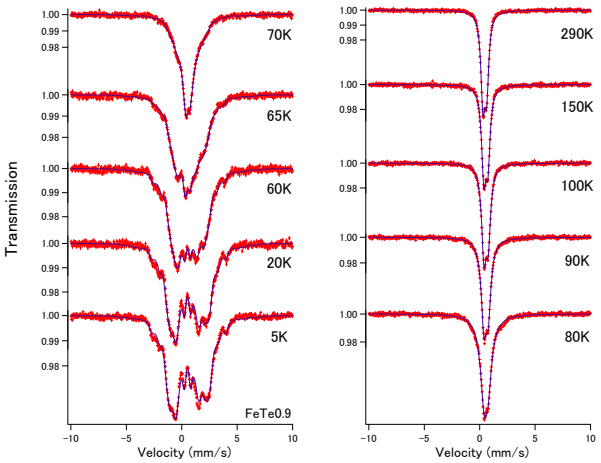

Fig. 1. Typical Mössbauer spectra for $FeTe_{0.9}$.

REFERENCES:

[1] Y. Kamihara, H. Hiramatsu, M. Hirano, R. Kawamura, H. Yanagi, T. Kamiya and H. Hosono, J. Am. Chem. Soc. **128** (2006)10012.
[2] Y. Kamihara, T. Watanabe, M. Hirano and H. Hosono, J. Am. Chem. Soc. **130** (2008) 3296.
[3] F.C. Hsu, J.Y. Luo, K.W. Yeh, T.K. Chen, T.W. Huang, P.M. Wu, Y.C. Lee, Y.L. Huang, Y.Y. Chu, D.C. Yan, and M.K. Wu, Proc. Natl. Acad. Sci. USA.**105** (2008) 14262.
[4]W. Bao, Y. Qiu, Q. Huang, M.A. Green, P. Zajdel, M.R. Fitzsimmons, M. Zhernenkov, S. Chang, M. Fang, B. Qian, E.K. Vehstedt, J. Yang, H.M. Pham, L. Spinu, and Z.Q. Mao, Phys. Rev. Lett. **102** (2009) 247001.
[5] S. Kitao, Y. Kobayashi, S. Higashitaniguchi, M. Saito, Y. Kamihara, M. Hirano, T. Mitsui, H. Hosono and M. Seto, J. Phys. Soc. Jpn. **77** (2008) 103706.
[6] S. Kitao, Y. Kobayashi, S. Higashitaniguchi, M. Kurokuzu, M. Saito, T. Mitsui, Y. Kamihara, M. Hirano, H. Hosono and M. Seto, J. Phys.: Conf. Ser. **217** (2010) 012120.
[7] J. Suwalski, J. Piekoszewski, and J. Leciejewicz, Proc. Conf. Appl. Möss. Effect 1969, p 385.
[8] Y. Mizuguchi, T. Furubayashi, K. Deguchi, S. Tsuda, T. Yamaguchi, and Y. Takano, Physica C **470** (Suppl. 1) (2010) S338.
[9] A. Błachowski, K. Ruebenbauer, P. Zajdel, E.E. Rodriguez and M.A. Green, J. Phys. Cond. Matter **24** (2012) 386006.

採択課題番号 24P3-6　メスバウアー分光を用いた新規材料の物性研究　プロジェクト
（京大・原子炉）瀬戸　誠、北尾真司、小林康浩

PR3-9 Study on Rapid Spin Equilibrium and Magnetic Phase Transition for $(C_6H_5)_4P[Mn^{II}Fe^{III}(C_2O_3S)_3]$ by Means of High Field ^{57}Fe Mössbauer Spectroscopy

N. Kojima, A. Okazawa, J. Yoshida, Y. Kobayashi[1] and M. Seto[1]

Graduate School of Arts and Sciences, The University of Tokyo
[1]Research Reactor Institute, Kyoto University

INTRODUCTION: In the case of assembled transition metal complexes whose spin states are in the spin-crossover region, concerted phenomena coupled with the spin-crossover phenomenon and magnetic phase transitions are expected. From this viewpoint, we have synthesized a mto (= C_2O_3S) bridged hetero-metal complex, $(C_6H_5)_4P[Mn^{II}Fe^{III}(mto)_3]$ (**1-mto**) consisting of $Fe^{III}O_3S_3$ and $Mn^{II}O_6$ octahedra [1]. In this complex, it is expected that the internal magnetic field at the Mn^{II} site is fluctuated by the rapid spin equilibrium at the Fe^{III} site, which influences the magnetic phase transition.

The molar magnetic susceptibility (χ_M) multiplied by the temperature, $\chi_M T$, is estimated at 6.90 cm^3 K mol^{-1} at 400 K. This value is in the middle of the spin-only values for the HS (S = 5/2) and LS (S = 1/2) states of Fe^{III}, 8.75 cm^3 K mol^{-1} and 4.75 cm^3 K mol^{-1}, respectively, implying that the spin equilibrium occurs at the $Fe^{III}O_3S_3$ site. The χ_M as a function of temperature has a broad maximum, a typical character of the 2D Heisenberg-type antiferromagnet, around 50 K, and shows a steep increase below 30 K with a hump around 23 K. At 23 K, both the real (χ') and imaginary (χ'') parts in the AC magnetic susceptibility exhibit steep peaks indicating a magnetic phase transition. At 30 K, the remnant magnetization and the magnetic hysteresis loop disappear. Therefore, it is obvious that **1-mto** undergoes two successive magnetic phase transitions at 30 K and 23 K. In order to investigate the rapid spin equilibrium and magnetic phase transition for **1-mto**, we performed ^{57}Fe Mössbauer spectroscopy under high magnetic fields.

EXPERIMENTS: The ^{57}Fe Mössbauer experiments on **1-mto** were carried out with a ^{57}Co/Rh source cooled down to 200 K using a superconducting magnet at the magnetic field up to 8 T. The magnetic field was applied parallel to the γ-ray direction. The spectra were calibrated by using the six lines of a body-centered cubic iron foil (α-Fe), the center of which was taken as zero isomer shift.

RESULTS: Fig. 1 shows the ^{57}Fe Mössbauer spectra of **1-mto** at 30 K, 22 K and 10 K. Despite the coexistence of HS and LS states of Fe^{III}, only a single doublet is observed between 300 and 30 K, which implies that the time scale of spin equilibrium between the HS and LS states is faster than that (10^{-7} s) of the ^{57}Fe Mössbauer spectroscopy between 300 and 30 K. At 30 K, despite the appearance of magnetic ordering, a single quadrupole doublet indicating a paramagnetic phase is observed. As temperature is lowered, a drastic change of the spectral profile caused by the internal magnetic field is seen between 23 K and 22 K, which reveals that the spin state at the Fe^{III} site is still paramagnetic even at 24 K, and both of the Mn^{II} and Fe^{III} spins are eventually ordered at about 23 K.

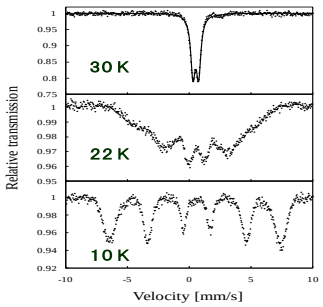

Fig. 1. ^{57}Fe Mössbauer spectra for **1-mto** at 30 K, 22 K, and 10 K [1].

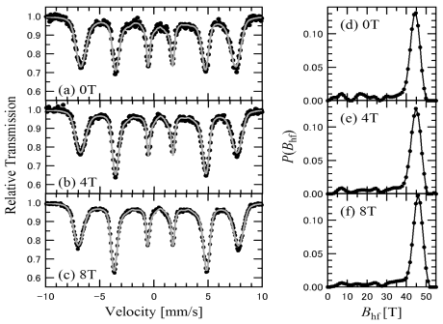

Fig. 2. Field dependence of the ^{57}Fe Mössbauer spectra for **1-mto** at 10 K (left). Hyperfine magnetic field distribution (right).

Fig. 2 shows the field dependence of the ^{57}Fe Mössbauer spectrum for **1-mto** at 10 K. In general, the relative line intensity of the ^{57}Fe Mössbauer line number of 2 and 5 depends on the angle, θ, between the Fe spin direction and the direction of the γ-ray from the Mössbauer source. The average angle, $\langle\theta\rangle$, is expressed as $\arccos\{(4 - x) / (4 + x)\}^{1/2}$, when the line intensity ratio is written as $3 : x : 1 : 1 : x : 3$. As shown in Fig. 2, the relative line intensity of the Mössbauer line no. of 2 and 5 increases in the order of H = 0 T → 4 T → 8 T as follows, 3 : 2.1 : 1 : 1 : 2.1 : 3 → 3 : 2.9 : 1 : 1 : 2.9 : 3 → 3 : 3.2 : 1 : 1 : 3.2 : 3. The $\langle\theta\rangle$ increases up to 70.1° with increasing external magnetic field up to 8 T, which implies that the critical field of spin-flop transition is higher than 8 T. Above the critical field, it is considered that the relative line intensity of the Mössbauer line no. of 2 and 5 decreases from 4 to 0 with increasing external filed. In order to investigate the anisotropic energy and the internal magnetic field, the high-field ^{57}Fe Mössbauer spectroscopy is indispensable and in progress.

REFERENCE:

[1] K. Kagesawa, Doctoral Thesis (The University of Tokyo, 2011).

採択課題番号 24P3-7　集積型 Fe(III)錯体におけるスピン平衡の強磁場下 ^{57}Fe　プロジェクト
メスバウアー分光研究

（東大・院総合文化）小島憲道、岡澤　厚、吉田順哉（京大・原子炉）小林康浩、瀬戸　誠

PR3-10 Elucidation of a Correlation between Magnetic Properties and Host-Guest Interactions in Porous Coordination Polymers

M. Ohba, R. Ohtani[1], M. Arai[1], S. Kitao[2] and M. Seto[2]

Department of Chemistry, Faculty of Science, Kyushu University
[1]Graduate School of Engineering, Kyoto University
[2]Research Reactor Institute, Kyoto University

INTRODUCTION:

Porous coordination polymers (PCPs) are a new type of guest adsorbent material consisting of flexible coordination bonds to provide permanent and designable regular porous structures [1]. Such PCPs are expected to be multifunctional platforms combining porous properties with specific chemical and physical properties. To couple magnetic or redox properties and the porous properties we synthesized two novel Fe(II) PCPs, {Fe(dpa)[Pt(CN)$_4$]G} (dpa = 1,2-di(4-pyridyl)ethane; G = dpa, stb (stilbene)) (**1-G**) and [Fe(isophthalate)(bpy)] (**2**). Host-guest composites, **1-G** accommodating some organic molecules as the guests, showed various spin transition (ST) behavior depending on the guest molecules. **1-dpa** showed a sharp three-step ST in 150-200 K, on the other hand, **1-stb** showed an abrupt one step ST. The guest-dependent ST behavior of **1-G** was explained by flexibility of the guest molecules. The multi-step ST of **1-dpa** was confirmed by ^{57}Fe-Mössbauer spectroscopy [2]. In the case of **2**, an encapsulation of iodine molecules induced a host-guest redox behavior [3]. The donor property of **2** had a strong interaction with the electron accepter iodine to form the donor-acceptor complex.

EXPERIMENTS: ^{57}Fe-Mössbauer spectroscopy was measured to use a ^{57}Co source with a nominal activity of 1.85 GBq. Velocity scale was calibrated as isomer shifts relative to α-Fe.

RESULTS: As shown in Fig. 1, the Mössbauer spectrum of **1-dpa** at 260 K consisted of a doublet peak with quadrupole splitting (ΔE_q) (0.90 m s^{-1}) and isomer shift (*IS*) (1.10 mm s^{-1}) and a singlet peak with *IS* (0.51 mm s^{-1}), in which the isomer shift was based on the value of α-Fe. These values of doublet and singlet peaks are typical for Fe^{II} ions in the HS (S = 2) and the LS (S = 0) states, respectively. The proportion of the HS state decreased with decreasing temperature; 90.2 % (at 260 K), 71.1 % (at 235 K), 53.6 % (at 220 K) and 13.3 % (at 100 K). The residual HS fraction at 100 K would be attributed to the generation of defects on the surface of microcrystals. Different ST behavior of **1-stb** were observed in Mössbauer spectra with IS of 0.46 (for singlet) and 1.15 (for doublet) and ΔE_q of 1.16 m s^{-1}. These results suggested that a slight difference in guest molecule greatly affects the magnetic behavior. In the case of **2**, all the iron species in the framework were determined to be Fe^{2+} by Mössbauer spectra. The framework possesses the electron donor property after degas treatment. **2** showed a permanent porosity and it adsorbed CO_2, N_2, and O_2 at 195 and 77 K. The donor property of **2** promoted the preferable iodine molecule insertion into the channel. The iodine-containing **2** was characterized by various spectroscopies and X-ray technique, and these elucidated that the half of Fe^{2+} were oxidized to Fe^{3+} and iodine were reduced. The hybrid of **2** and iodine showed over 10^{-5} S/cm of electron conductivity.

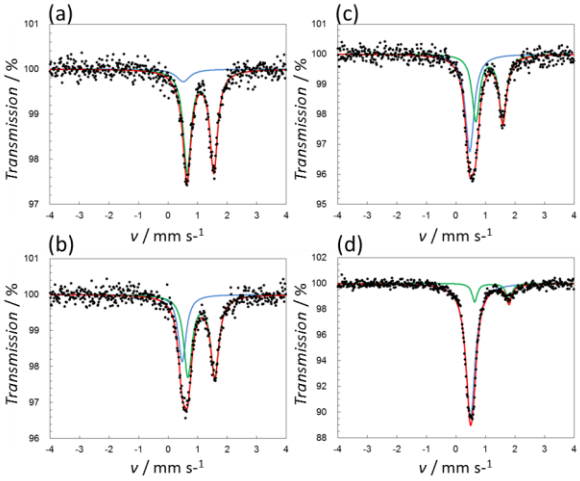

Fig. 1. ^{57}Fe-Mössbauer spectra of **1-dpa** measured at (a) 260 K, (b) 235 K, (c) 220 K, (d) 100 K in the heating process.

REFERENCES:

[1] S. Kitagawa *et al.*, *Angew. Chem. Int. Ed.*, 43 (**2004**) 2334-2375.
[2] R. Ohtani, M. Arai, S. Kitao, M. Seto, S. Kitagawa, M. Ohba *et al.*, *J. Inorg. Organomet. Polym. Mater.* 23 (**2013**) 104-110.
[3] S. Horike, M. Sugimoto, S. Kitao, M. Seto, S. Kitagawa *et al.*, *J. Mater. Chem. A.* 1, (**2013**) 3675-3679.

採択課題番号 24P3-8 多孔性金属錯体におけるホストーゲスト相互作用と磁気特性の相関の解明　　プロジェクト

（九大院・理）大場正昭（京大院・工）大谷　亮、荒井将司（京大・原子炉）北尾真司、瀬戸　誠

PR3-11

Characterization of Gold Clusters Supported on Zinc Oxide by ^{197}Au Mössbauer Spectroscopy

T. Yokoyama, Y. Okaue, D. Kawamoto, H. Ohashi[1], Y. Kobayashi[2] and S. Kitao[2]

Faculty of Sciences, Kyushu University
[1]Faculty of Arts and Science, Kyushu University
[2]Research Reactor Institute, Kyoto University

INTRODUCTION: Gold nanoparticles supported on zinc oxide have been used as various oxidation-reduction catalysts. It is essential to characterize the catalysts for understanding their advantages and establishing the guidelines for synthesizing catalysts with high activity. For the characterization of supported gold catalysts, their oxidation states have been determined by X-ray absorption spectroscopy (XAS) and the crystal phases have been detected by powder X-ray diffraction (XRD). However, supported gold catalysts have rarely been characterized by ^{197}Au Mössbauer spectroscopy.

In this study, the detailed chemical states of supported gold catalysts were elucidated based on a combination of XAS and ^{197}Au Mössbauer spectroscopy.

EXPERIMENTS: Supported gold catalysts（Au/ZnO）were prepared by the coprecipitation method. An aqueous mixed solution of $HAuCl_4$ and $Zn(NO_3)_2$ was poured into an NaOH solution under stirring. The pricipitate was filtered, washed and freeze dried. The obtained materials were calcined in air（Au/ZnO (air)）or were reduced in a flow of H_2 gas（Au/ZnO (H_2)）at 573 K for 4 h.

The chemical state of Au in the solid samples was determined by ^{197}Au Mössbauer spectroscopy (home-made equipment). ^{197}Pt isotopes ($T_{1/2}$ = 18.3 h), a γ-ray source feeding the 77.3-keV Mössbauer transition of ^{197}Au, were prepared by neutron irradiation of isotopically enriched ^{196}Pt metal at the Kyoto University Reactor. The absorbers were the particle specimens. The source and specimens were cooled with a helium refrigerator. The temperature of the specimens was in the range 8 – 15 K. The zero velocity point of the spectra was taken to be the peak point for pure bulk gold. The spectra for all the solid samples were each fitted with a single Lorentzian function.

Furthermore, for these catalysts, the Zn-K edge and Au-L_3 edge XAS were measured at BL14B2 of SPring-8(Hyogo, Japan).

RESULTS: The Zn-K XANES spectra for the Au/ZnO(air) and Au/ZnO (H_2) catalysts revealed that Zn was not reduced, unlike Ni in an Au/NiO (H_2) catalyst. The Au-L_3 XANES spectra for the Au/ZnO (H_2) catalyst confirmed the presence of Au(0). However, the Au(0) was different from the bulk Au, suggesting a formation of gold clusters. Fig. 1 shows the ^{197}Au Mössbauer spectra for the Au/ZnO catalysts. From the ^{197}Au Mössbauer spectrum for Au/ZnO (H_2), it can be reasonably expected that relatively-uniform clusters were formed by hydrogen reduction. After all, our established approach of the combination of XAS and ^{197}Au Mössbauer spectroscopy [1] is quite useful to characterize supported gold catalysts.

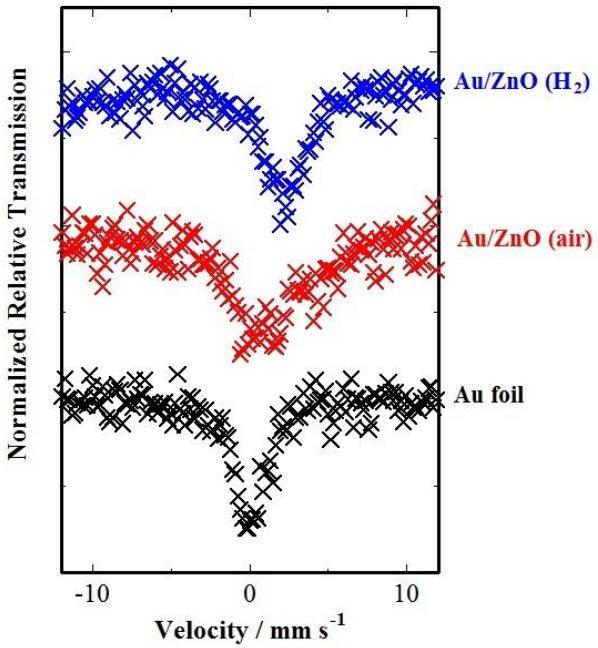

Fig. 1. ^{197}Au Mössbauer spectra for Au/ZnO catalysts and Au foil.

REFERENCE:

[1] D. Kawamoto *et al.*, *Adv. X-Ray. Chem. Anal., Japan*, **43**, pp.293-302 (2012).

採択課題番号 24P3-9　メスバウアー分光による金触媒中の金化学種の状態分析　　プロジェクト
（九大院・理）横山拓史、岡上吉広、川本大祐　（九大・基幹教育院）大橋弘範
（京大・原子炉）小林康浩、北尾真司

PR3-12 ^{129}I Mössbauer Spectroscopy of AgI Nanoparticles

T. Yamamoto, K. Otsubo, H. Kitagawa, S. Kitao[1] and M. Seto[1]

Graduate School of Science, Kyoto University
[1]Research Reactor Institute, Kyoto University

INTRODUCTION: Solid-state ionic conductors have been actively studied in many fields of science and technology because of their properties and application. Although liquid phases exhibit high ionic conductivity, solid-state ionic conductors are much more desirable from the viewpoint of application for electrochemical devices such as batteries [1] and sensors (device fabrication, stability and safety). One of the highest conductive ionic conductors is silver iodide (AgI) [2], which shows superionic conductivity greater than 1 S cm^{-1} in the high-temperature α-phase [3]. Below 147 ℃, AgI undergoes a phase transition into a mixture of poorly conducting β- and γ-phases, which limits its application. Recently methods for the preparation of AgI nanoparticles have been reported and phase behavior has been investigated [4-7]. With decreasing nanoparticles size, the temperature of α- to β-/γ- phase transition shifts lower, for instance, the α-phase survives down to 37 °C in 6.3-nm AgI nanoparticles. However, the origin of stabilization of the α-phase is not clear. So, here we report ^{129}I Mössbauer spectroscopy of AgI nanoparticles, and discuss the correlation between stabilization and interaction of interface.

EXPERIMENTS: The sample used was synthesized by the solution method. In order to avoid photoreduction of AgI, the synthesis was carried out with an apparatus covered with aluminum foil. $AgNO_3$ (0.067 mmol) and poly-N-vinyl-2-pyrrolidone (PVP) K30 (1.243 mmol) were dissolved in 60 mL of cold methanol and stirred at the ice temperature for several minutes. Then 3.4 mL of Na^{129}I aqueous solution (1.61 μCi / mL) was added quickly and stirred for 2 h. The synthesized sample was collected by centrifugation and dried in air.

^{129}I Mössbauer spectroscopy on the synthesized sample was performed at 13 K. ^{66}Zn^{129}Te was used as the γ-ray source, which was prepared by neutron irradiation of ^{66}Zn^{128}Te. The source velocity was calibrated by using pure α-Fe as the control material.

RESULTS: The observed data (dots) and the fitting line are shown in Fig. 1. The fitting gives the hyperfine interaction parameters (isomer shift IS, line width *W*, quadrupole coupling constant QCC, and asymmetry parameter η). IS is 0.01 mm/s relative to the ^{66}Zn^{129}Te source. The slightly large *W* value (1.65 mm/s) indicates that QCC has some distribution, and QCC is estimated at -426.6 MHz. Interestingly, the fitting gives better results with taking η as 0.62 rather than zero. From these parameters, it is supposed that the iodine in the AgI nanoparticles has a charge slightly more positive than -1, although that in bulk AgI has -1. It is conceivable that this charge change derives from an interaction between the surface of the nanoparticles and PVP. This strong interaction changes the surface energy of the nanoparticles, which can result in stabilization of the α-phase.

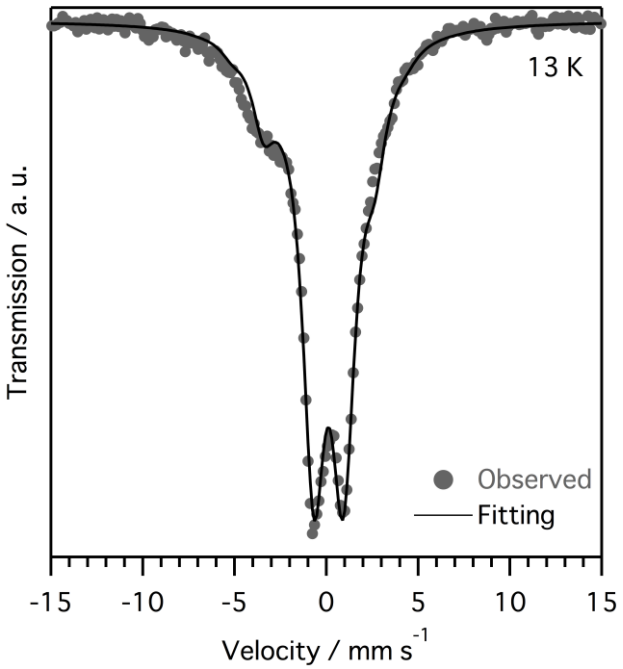

Fig. 1. The ^{129}I Mössbauer spectrum for AgI nanoparticles using a Zn^{129}Te source. The obtained hyperfine interaction parameters are IS = 0.01 mm/s, *W* = 1.65 mm/s, QCC = -426.6 MHz, and η = 0.62.

REFERENCES:

[1] B. B. Owens, J. Power Sources, **90** (2000) 2-8.
[2] Z. Tubandt and E. Lorenz, Z. Phys. Chem., **87** (1914) 513-542.
[3] S. Hull, Rep. Prog. Phys., **67** (2004) 1233-1314.
[4] R. Makiura, T. Yonemura, T. Yamada, M. Yamauchi, R. Ikeda, H. Kitagawa, K. Kato and M. Takata, Nat. Mater., **8** (2009) 476-480.
[5] S. Yamasaki, T. Yamada, H. Kobayashi and H. Kitagawa, Chem. Asian J., **8** (2013) 73-75.
[6] W. Sun, Y. Li, W. Shi, X. Zhao and P. Fang, J. Mater. Chem., **21** (2011) 9263-9270.
[7] B. Xu and X. Wang, Small, **7** (2011) 3439-3444.

採択課題番号 24P3-10　　ヨウ化銀ナノ粒子の相挙動の評価　　プロジェクト
（京大院・理）北川　宏、山田鉄平、大坪主弥、小林浩和、貞清正彰、山本貴之（京大・原子炉）北尾真司、瀬戸　誠